

VU Research Portal

A contribution to the study of the economic causes and consequences of climate change:

Estrada Porrua, F.

2015

document version

Publisher's PDF, also known as Version of record

[Link to publication in VU Research Portal](#)

citation for published version (APA)

Estrada Porrua, F. (2015). *A contribution to the study of the economic causes and consequences of climate change: An interdisciplinary approach*. [PhD-Thesis - Research and graduation internal, Vrije Universiteit Amsterdam].

General rights

Copyright and moral rights for the publications made accessible in the public portal are retained by the authors and/or other copyright owners and it is a condition of accessing publications that users recognise and abide by the legal requirements associated with these rights.

- Users may download and print one copy of any publication from the public portal for the purpose of private study or research.
- You may not further distribute the material or use it for any profit-making activity or commercial gain
- You may freely distribute the URL identifying the publication in the public portal

Take down policy

If you believe that this document breaches copyright please contact us providing details, and we will remove access to the work immediately and investigate your claim.

E-mail address:

vuresearchportal.ub@vu.nl

8 Climate change impact functions with adaptation and dynamic sensitivity

Through stylized damage functions, Integrated Assessment Models (IAMs) provide estimates of the economic costs that would occur for absolute changes in global temperature. We propose a new type of damage functions that allows mapping economic losses in terms of how extreme global temperature changes are in relation to a coping range representing the capacity of a system to deal with the climate conditions experienced at a particular period of time. In these new damage functions, adaptation to a changing climate is introduced by allowing the reference climate to be a function of time instead of a fixed quantity. Different formulations of impact functions discussed in the literature arise as special cases.

8.1 Introduction

The function that relates climate change to its impacts is crucial for any assessment of the seriousness of climate change. Integrated Assessment Models often use stylized impact functions with implicit adaptation and fixed sensitivity for all warming trajectories. We here propose a tractable generalization with adaptation and sensitivity made explicit.

The most common impact function in Integrated Assessment Models (IAMs) is a polynomial function of global temperature (e.g., Warren et al. 2006):

$$D_t = \alpha_1 T_t + \alpha_2 T_t^{\alpha_3} \quad (8.1)$$

This paper is based on Estrada F., Tol R.S.J. Generalized impact functions based on dynamic coping ranges and adaptation. In preparation.

where D_t are the damages due to changes in global or regional temperatures (T_t) with respect to a reference period (frequently the pre-industrial climate) and α_1 , α_2 , α_3 are fixed parameters calibrated for a certain increase in global temperature (e.g., 2.5°C or a doubling of the atmospheric concentration of CO₂) and frequently $\alpha_3 = 2$.

In general, impacts can be conceptualized as a function of changes in climate (hazard), sensitivity, and adaptive capacity. In an equation such as (8.1) these three determinant factors and their interactions are combined in an intractable way (e.g., Tol and Fankhauser 1998; Tol, Fankhauser, and Smith 1998; Patt et al. 2010; Fussel 2010). In this chapter we present a generalized impact function based on a transformation that "standardizes" changes in climate by means of the system's coping range and adaptive capacity. The system's sensitivity and adaptive capacity are dynamic and explicit in this new impact function. Economic losses are mapped in terms of the capacity of a system to deal with climate conditions at a certain period in time, instead of absolute changes in climate variables as is done by current IAMs.

The chapter is structured as follows. Section 8.2 presents a generalization of the impact functions. In Section 8.3 some of the impact functions commonly referred in the literature are recalibrated for accommodating the modifications proposed in Section 8.2 and for discussing the underlying implications of current impact functions in IAM. The conclusions and future extensions are presented in Section 8.4.

8.2 A generalization of impact functions

Consider the following generalization of the impact function in equation (8.1):

$$D_t^{ad} = \alpha_1 S_t + \alpha_2 S_t^{\alpha_3} \quad (8.2)$$

where

$$S_t = \frac{T_t - a_t}{\sigma_t} \quad (8.3)$$

and σ_t represents the coping range of the system which is a measure of its sensitivity to changes in T_t . a_t represents the current level of adaptation to movements in T_t . Both σ_t and a_t are expressed in °C and S_t is measured in coping range units. Note that the "standardization" of T_t in equation (8.3) is not conducted to reflect the statistical properties of T_t . In this re-expression, the impacts become a function of how extreme the climate conditions are for a given system with particular coping and adaptation capacities, instead of absolute temperature changes²⁸.

Through adaptation, the system can migrate to a new set of normal climate conditions. In this way, the climate of reference in equations (8.2) and (8.3) above is time-dependent, and the damage function thus changes over time too.

From (8.2) and (8.3) we have

$$D_t^{ad} = \frac{\alpha_1}{\sigma_t} (T_t - a_t) + \frac{\alpha_2}{\sigma_t^{\alpha_3}} (T_t - a_t)^{\alpha_3} = \beta_{1,t} (T_t^*) + \beta_{2,t} (T_t^*)^{\alpha_3} \quad (8.4)$$

Making σ_t a function of time is equivalent to having an impact function with time-varying parameters, which reflects changes in the sensitivity of the system to net changes in temperature (T_t^*).

If a regional dimension is considered, equation (8.4) can be generalized to

²⁸ For the ease of exposition and without any loss in generality, we assume that deviations with respect to the optimal climate generate negative impacts and that the impacts under the optimum temperature are zero. Note that any power or polynomial function can be shifted in this way by adding a constant.

$$D_{r,t}^{ad} = \frac{\alpha_1}{\sigma_{r,t}} (T_{r,t} - a_{r,t}) + \frac{\alpha_2}{\sigma_{r,t}^{\alpha_3}} (T_{r,t} - a_t)^{\alpha_3} = \beta_{1,r,t} (T_{r,t}^*) + \beta_{2,r,t} (T_{r,t}^*)^{\alpha_3} \quad (8.5)$$

where the coefficients of the r regions are explicitly scaled by their sensitivity, giving an alternative approach for producing regional models (see Appendix E for an example).

The adaptation function can be represented as the sum of planned and autonomous adaptation at time t :

$$a_t = \phi_{1,t} + \phi_{2,t} \quad (8.6)$$

where $\phi_{1,t}$ and $\phi_{2,t}$ represent planned and autonomous adaptation, respectively. As such $\phi_{1,t}$ is a decision variable. Two possible specifications are proposed for the autonomous adaptation:

$$\phi_{2,t} = T_t e^{-T_t} \quad (8.7a)$$

and

$$\phi_{2,t} = T_t e^{-(T_t - \phi_{1,t})} \quad (8.7b)$$

In both equations (8.7a) and (8.7b) the autonomous adaptation capacity is a decreasing function of T_t where $T_t \geq 0$ ²⁹. For small changes in climate the value of exponential weighting function in these equations is close to 1 and therefore the $\phi_{2,t} \approx T_t$. However, as T_t increases, the capacity of the system to adapt in an autonomous and costless way decreases. This specification assumes that as the system gets increasingly stressed due to the changes in climate, its capacity to respond autonomously is reduced. Equation (8.7b)

²⁹ To allow for negative temperature changes $T_t e^{-|\cdot|}$ can be used.

allows for synergistic effects between planned and autonomous adaptation by reducing the rate at which autonomous adaptation decreases with increases in T_t . The rationale behind equation (8.7b) is that planned adaptation is likely to provide favorable conditions for further autonomous adaptation to take place.

As in previous studies (K. C. de Bruin, Dellink, and Tol 2009; K. de Bruin, Dellink, and Agrawala 2009), the adaptation costs are assumed to be a power function of $\phi_{1,t}$:

$$AD_t = \lambda_1 \phi_{1,t}^{\lambda_2} \quad (8.8)$$

The optimality conditions for $\phi_{1,t}$ can be obtained by maximizing the net benefits of planned adaptation in terms of avoided damages i.e., the difference in damages due to adaptation minus the costs of adaptation in time t :

$$NB_t = D_t(T_t) - D_t^{ad}(T_t, a_t) - AD_t = \beta_1 T_t + \beta_2 T_t^{\alpha_3} - [\beta_1 (T_t - a_t) + \beta_2 (T_t - a_t)^{\alpha_3}] - \lambda_1 \phi_{1,t}^{\lambda_2} \quad (8.9)$$

which can be simplified to:

$$NB_t = \beta_2 T_t^{\alpha_3} + \beta_1 a_t - \beta_2 (T_t - a_t)^{\alpha_3} - \lambda_1 \phi_{1,t}^{\lambda_2}$$

where a_t is restricted to values $a_t \geq 0$. The upper limit for the optimal value of $\phi_{1,t}$ value is given by the inequality $\beta_1 a_t + \beta_2 T_t^{\alpha_3} - \beta_2 (T_t - a_t)^{\alpha_3} \leq \lambda_1 \phi_{1,t}^{\lambda_2}$. The optimal values for $\phi_{1,t}$ are shown below for three different cases of autonomous adaptation:

Case 1. No autonomous adaptation $a_t = \phi_{1,t}$.

$$\frac{\partial NB_t}{\partial \phi_{1,t}} = \beta_1 + \alpha_3 \beta_2 (T_t - \phi_{1,t})^{\alpha_3 - 1} - \lambda_2 \lambda_1 \phi_{1,t}^{\lambda_2 - 1} = 0 \quad (8.10a)$$

Case 2. Planned and autonomous adaptation $a_t = \phi_{1,t} + \phi_{2,t} = \phi_{1,t} + T_t e^{-T_t}$.

$$\frac{\partial NB_t}{\partial \phi_{1,t}} = \beta_1 + \alpha_3 \beta_2 (T_t - (\phi_{1,t} + \phi_{2,t}))^{\alpha_3 - 1} - \lambda_2 \lambda_1 \phi_{1,t}^{\lambda_2 - 1} = 0 \quad (8.10b)$$

Case 3. Synergistic effects between planned and autonomous adaptation

$$a_t = \phi_{1,t} + \phi_{2,t} = \phi_{1,t} + T_t e^{-(T_t - \phi_{1,t})}.$$

$$\frac{\partial NB_t}{\partial \phi_{1,t}} = \beta_1 + \alpha_3 \beta_2 (1 + \phi_{2,t}) (T_t - (\phi_{1,t} + \phi_{2,t}))^{\alpha_3 - 1} - \lambda_2 \lambda_1 \phi_{1,t}^{\lambda_2 - 1} = 0 \quad (8.10c)$$

There is no analytical solution to any of these three first-order conditions. Figure E1 provides an example of the optimal adaptation levels for the three cases above and for particular parameter values and different increases in T_t . This figure shows an interesting aspect of the interaction between autonomous and planned adaptation: for moderate warming, autonomous adaptation can have opposite effects over the optimal level of planned adaptation that is chosen. If autonomous and planned adaptation are independent, the introduction of autonomous adaptation leads to lower levels of optimal planned adaptation. In contrast, if synergistic effects are allowed between the two types of adaptation, the resulting optimal level of planned adaptation is higher when autonomous adaptation is included.

The coping range defines the interval within which variations in climate conditions do not cause significant impacts to a system due to its underlying resilience (see Yohe and Tol 2002; Downing et al. 1997). The coping range is not necessarily constant, and therefore the same climate shock can cause different impacts depending on the state of the system. Moreover, significant and/or sustained impacts to the system can decrease its resilience and capacity to cope in the following periods. The dynamics of the coping range can be represented as follows:

$$\sigma_t = \mu + \rho\sigma_{t-1} - D_{t-1}^{ad}\sigma_{t-1} = \mu + \rho_t^*\sigma_{t-1} \quad (8.11)$$

for $t = 1, \dots, T$, $\sigma_t > 0$ and $\sigma_0 = \sigma^*$ is the optimal, undisturbed coping range of the system and $\mu = (1 - \rho)\sigma^*$. Note that σ_t depends on a_{t-1} via D_{t-1}^{ad} but it is independent from a_t . Equation (8.11) can be rewritten as

$$\sigma_t = (1 - \rho)\sigma^* + \rho_t^*\sigma_{t-1}$$

which shows that the coping range at time t is an average of the undisturbed coping range and the coping range at time $t-1$, weighted by ρ^* and $(1 - \rho)$. Under stationary climate conditions $\sigma_t = \sigma^*$. However, under changing climate conditions D_{t-1}^{ad} will be systematically different from zero and the coping range will decrease/increase as the impacts of climate change become more negative/positive. This implies that the sensitivity of the system —represented by the parameters in equation (8.4)— will change accordingly to reflect the time-evolving coping capacity of the system. In addition, the effects of D_{t-1}^{ad} on σ_t are persistent and even when the direct impacts of climate change have stopped, the system will only go back to its original state after a certain period of time. The effects of a shock c on σ_t will be more persistent as ρ approaches 1, given that $\sigma_t = \sigma^* + \rho^{t-1}c\sigma^*$ for $t \geq 1$.

While σ^* is a description of the initial state of the system's vulnerability, σ_t is determined in part by a_{t-1} . The effects of adaptation over the coping range are³⁰:

$$\frac{\partial \sigma_t}{\partial a_{t-1}} = \beta_{1,t-1}\sigma_{t-1} + \alpha_3\beta_{2,t-1}\sigma_{t-1}(T_{t-1} - a_{t-1})^{\alpha_3-1} \quad (8.12)$$

³⁰ Note that $\frac{\partial \sigma_t}{\partial a_t} = 0$ i.e., the coping range does not depend on a_t .

Once the coping range is dynamic, the adaptation chosen in $t-1$ affects the net benefits of adaptation $NB_t = D_t(T_t, \sigma_0) - D_t^{ad}(T_t, a_t, \sigma_t) - AD_t$ as follows:

$$\frac{\partial NB_t}{\partial a_{t-1}} = \frac{\partial \beta_{1,t}}{\partial a_{t-1}} (T_t - a_t) + \frac{\partial \beta_{2,t}}{\partial a_{t-1}} (T_t - a_t)^{\alpha_3} \quad (8.13)$$

where

$$\frac{\partial \beta_{1,t}}{\partial a_{t-1}} = \beta_{1,t-1} \frac{\sigma_{t-1}^2}{\sigma_t^2} \frac{\partial D_{t-1}^{ad}}{\partial a_{t-1}}$$

$$\frac{\partial \beta_{2,t}}{\partial a_{t-1}} = 2\beta_{2,t-1} \frac{\sigma_{t-1}^3}{\sigma_t^3} \frac{\partial D_{t-1}^{ad}}{\partial a_{t-1}}$$

That is, the change in NB_t produced by a_{t-1} is determined by the changes in the coefficients $\beta_{1,t}$ and $\beta_{2,t}$. These changes are a function of the coefficient values in the previous period, the change in damages due to the change in a_{t-1} , and a sensitivity scaling factor involving the ratio of the coping range values in periods t and $t-1$.

Finally, equations (8.4) and (8.5) can also be generalized to be stochastic by allowing the coping range to be a random variable in order to reflect the intrinsic uncertainty regarding the resilience/sensitivity of the system. Impact functions similar to those in the PAGE2002 model (Hope 2006) arise as a special case when parameters are assumed to be time-invariant.

8.3 Generalizing the DICE and AD-DICE impact functions to include dynamic coping ranges and adaptation.

8.3.1 Standard impact functions

The DICE impact functions (Nordhaus and Boyer 2000; Nordhaus 2008) express damages in terms of changes in global temperature from its 1900 value, which is chosen to represent the pre-industrial climate. We use the global temperatures from the HadCRUT4 dataset³¹ to characterize this baseline climate. The parameter values for DICE99, DICE2007 and AD-DICE2007 (gross damage) are shown in Table 8.1 as well as a version of AD-DICE2007 impact function (K. de Bruin, Dellink, and Agrawala 2009; K. C. de Bruin, Dellink, and Tol 2009) with an integer power ($\alpha_3 = 2$). This modified version of the AD-DICE2007 was calibrated by minimizing the sum of square differences between the original and modified functions for a range of 0°C to 6°C temperature increase ($R^2 = 0.997$). The main difference between the DICE and AD-DICE2007 impact functions is that the first is calibrated to represent expected impacts after "optimal adaptation", while that of the AD-DICE2007 is calibrated to reproduce the implied total damages (i.e., the impacts after adaptation plus adaptation costs) of the DICE model.

Table 8.1. Parameter values of the damage functions in the original and modified DICE99 and DICE2007 models.

Model	α_1	α_2	α_1^{cr}	α_2^{cr}	Power
DICE99	-0.00450	0.00350	-0.00155	0.00042	2
DICE2007	0.00000	0.00284	0.00000	0.00034	2
AD-DICE2007 (Gross damage)	0.0004	0.0027	0.00014	0.00025	2.243
AD-DICE2007* (Gross damage)	--	--	0.00000	0.00057	2

It is straightforward to calibrate Equation (8.4) to reproduce the results of the DICE-type impact functions:

$$D_t^{\text{mod}} = \alpha_1 \sigma S_t + \alpha_2 \sigma^2 S_t^2 = \alpha_1^{cr} S_t + \alpha_2^{cr} S_t^2 \quad (8.14)$$

For this calibration an estimate of the coping range is needed. One possibility is to choose σ such that the world was nearly completely adapted to the pre-industrial climate by

³¹ <http://www.metoffice.gov.uk/hadobs/crutem4/>

year 1900, although this might be an overly optimistic assumption. As such, assume that the coping range corresponds to 3 standard deviations of global temperatures estimated from a 30-year period centered in 1900³². The coping range is $\sigma^* = 0.35^\circ\text{C}$ and the calibrated parameters are shown in Table 8.1. Note that the magnitude of σ^* is deceptively small. Such value at the global scale implies much larger variability at regional and local scales and therefore a coping range of 0.35°C can be indeed large for the world's societies and natural systems as a whole (Figure 8.1).

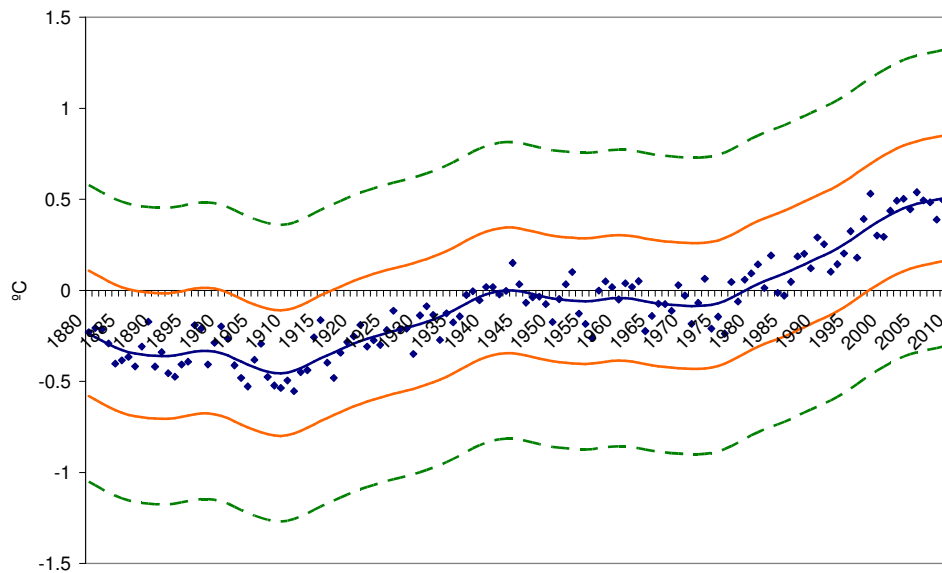


Figure 8.1. Global temperatures and coping ranges. The solid blue line shows the smoothed temperatures using the Hodrick-Prescott filter. The orange and the dotted green lines denote the mean plus/minus 3 standard deviations for a centered 30-year period around 1900 and for the whole sample, respectively.

Table 8.2 shows what increases up to 6°C in global temperature represent in coping range units and the corresponding expected economic impacts according to the DICE models. Making an analogy with statistical concepts helps illustrating the magnitude of the projected changes. Assume the coping range to be the standard deviation of a Normal distribution. A three standard deviation change in the mean conditions would take the system out of a large part of what it had previously experienced and for a six standard

³² Global temperature during the selected period can be represented by a Normal distribution (Jarque-Bera statistic 1.93). An interval of three standard deviations from the mean covers about 99.7% of the probability mass of this distribution.

deviation change there would be virtually no overlapping between the past and future probability distributions.

As shown in Table 8.2, a near six σ^* change would occur for a 2°C increase in T_t and a 6°C change would entail taking the system out of its normal conditions by more than 17 times σ^* . The corresponding economic impacts projected by the DICE99 (DICE2007) and AD-DICE2007 (modified AD-DICE2007) models are about 0.5% (1.14%) and 9.9% (10.22%) for a 2°C warming and about than 1.36% (1.92%) and 15.26% (17.26%), respectively, for 6°C. It is hard to imagine any natural or social system that, when taken so far outside the set of conditions it has ever experienced, would suffer so little damage. As such, Table 8.2 suggests that as has been previously pointed out (Weitzman 2012), these impact functions may importantly underestimate the potential damages of climate change, particularly for large increases in T_t . As shown by the numbers in brackets in Table 8.2, these arguments hold even when a much larger value for the coping range is chosen ($\sigma^* = 0.81$, three standard deviations of T_t estimated using the whole sample period 1850-2010; see Figure 8.1).

Table 8.2. Projected impacts for global temperature increases from 0°C to 6°C.

T_t (°C)	T_t (σ^*)	DICE99	DICE2007	AD-DICE2007 (Gross damage)	AD-DICE2007* (Gross damage)
0	0	0	0	0	0
1	2.90 [1.24]	0.10	-0.28	-0.31	-0.48
2	5.80 [2.48]	-0.50	-1.14	-1.36	-1.92
3	8.70 [3.72]	-1.80	-2.56	-3.29	-4.31
4	11.59 [4.97]	-3.80	-4.54	-6.21	-7.67
5	14.49 [6.21]	-6.50	-7.10	-10.18	-11.98
6	17.39 [7.45]	-9.90	-10.22	-15.26	-17.26

8.3.2 Generalized impact function

The planned adaptation costs function in equation (8.8) was calibrated by minimizing the sum of the square differences between the original costs function (K. C. de Bruin, Dellink, and Tol 2009) and equation (8.8). The calibration point chosen was 2.4°C

increase over the 1900 value. The parameter values for equation (8.8) are $\lambda_1 = 11.712$ and $\lambda_2 = 4$ and as shown in Figure E2, the costs for adapting to small changes in T_t are very low but rapidly accelerate for larger values of $\phi_{1,t}$, reaching 1% of GDP for about 0.5°C and about 11.7% for 1°C.

To illustrate the proposed generalized impact function, we use two arbitrary climate change scenarios consisting in linear increases in global temperature of 2°C and 6°C, respectively, in 100 years. For these examples, world GDP is assumed to grow exponentially at a 2% rate. To obtain the optimal adaptation effort, an optimization procedure for maximizing the present value of GDP (at a 4% discount rate) was applied. The coping range dynamic equation (8.11) is parameterized to represent two different cases: low ($\rho = 0$) and high ($\rho = 0.5$) sensitivities.

First we discuss the case of no autonomous adaptation ($a_t = \phi_{1,t}$). Figure 8.2 compares the economic impacts as percent of global GDP obtained from the modified AD-DICE2007 impact function to those from the generalized impact function described in the previous section. Panels a) and b) show that for moderate changes in T_t (i.e., 2°C), the projected impacts from the proposed impact function are almost the same as those of the AD-DICE2007 (i.e., show a similar quadratic-type behavior), irrespective if the sensitivity of the coping range is low or high. The optimal adaptation produces important reductions in damages of almost one-quarter of the expected gross impacts and leads to values similar to the original DICE2007 "optimal adaptation" function.

In contrast, for large increases in temperature (panels a and b) the projected impacts from the generalized impact function are highly nonlinear and very different to those of the AD-DICE2007. The sensitivity of the coping range has a large impact on the percent of GDP loss. In fact, panel d) shows damages comparable to those in Weitzman (Weitzman 2012) but in this case arising as a consequence of past climate change impacts over the coping capacity of the system.

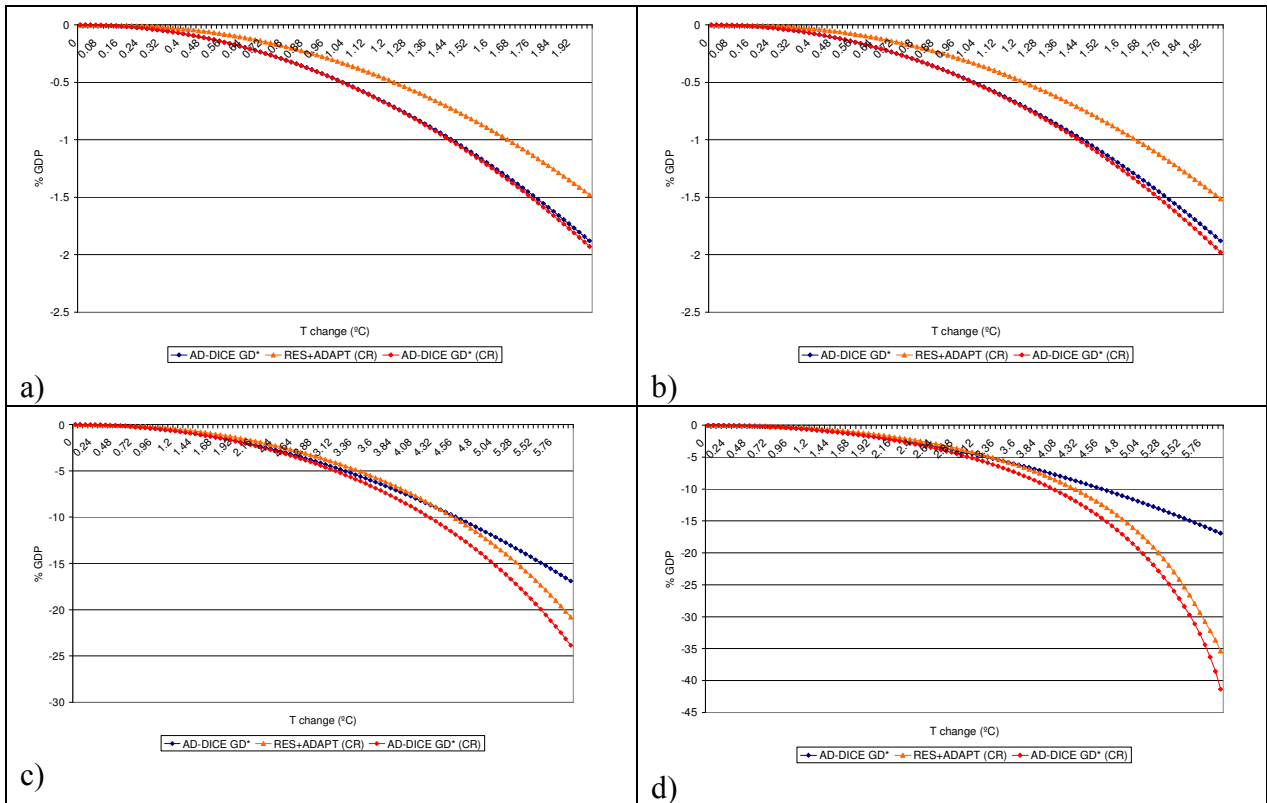


Figure 8.2. Economic losses as percent of global GDP. Panels a) and b) show the projected losses for a 2°C increase in T_l for low and high sensitivity, respectively. Panels c) and d) show the projected losses for a 6°C increase in T_l for low and high sensitivity, respectively. . AD-DICE GD*, RES+ADAPT (CR) and AD-DICE GD (CR) represent the Modified AD-DICE gross damage impact function, the residual and adaptation costs using a dynamic coping range and the AD-DICE gross damage using a dynamic coping range, respectively.

The optimal adaptation level and the corresponding costs for the different climate scenarios and sensitivities are shown in Figure 8.3 panels c) and d). These panels illustrate how for large changes in T_l the sensitivity of the coping range can introduce large nonlinearities to the optimal adaptation path and its costs, while for small changes in climate the differences between high and low sensitivity estimates are negligible. The costs of adaptation for the 2°C temperature scenario increase slowly and reach about one tenth of percent of global GDP at the end of the century, irrespective if a low or high sensitivity is chosen. However, the differences in adaptation costs from low to high sensitivities under the more extreme climate change scenario are very large representing up to 5% of GDP. It is also interesting to note that for this scenario, the adaptation levels

at the end of the century drop given that the benefits of adaptation in terms of reduced impacts no longer justify the costs of maintaining it. After this point, GDP stops growing and, in the case of high sensitivity and no adaptation, it actually decreases (Figure E3).

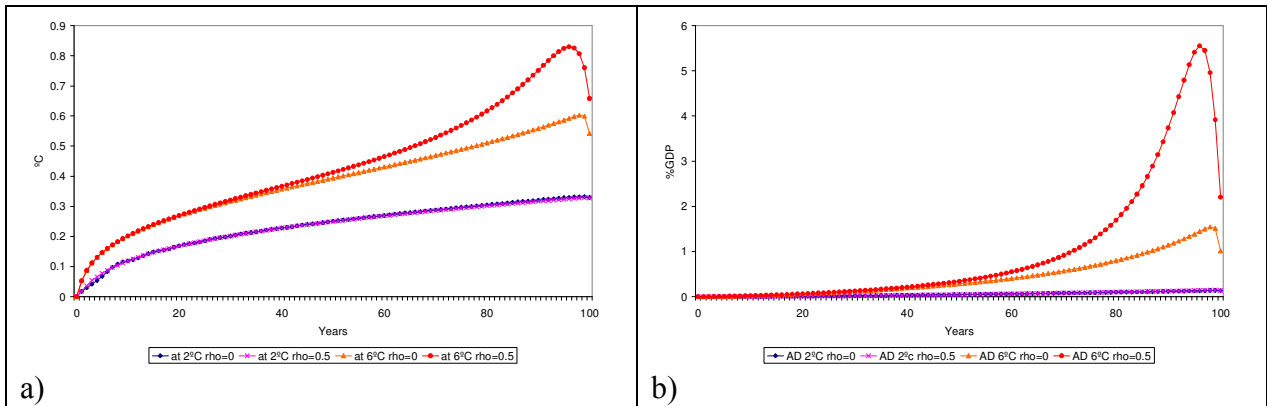


Figure 8.3. Panel a) adaptation level a_t for $T_t = 2^\circ C$, low and high sensitivity (blue and pink lines, respectively) and $T_t = 6^\circ C$, low and high sensitivity (orange and red lines, respectively). Panel b) adaptation costs AD_t for $T_t = 2^\circ C$, low and high sensitivity (blue and pink lines, respectively) and $T_t = 6^\circ C$, low and high sensitivity (orange and red lines, respectively)

8.3.3 Autonomous adaptation

We now turn to the cases in which autonomous adaptation is included by means of equations (8.7a) and (8.7b). Results are based on the same climate scenarios described above and high sensitivity in the coping range specification ($\rho = 0.5$). Under a moderate warming scenario (Figure 8.4a), the introduction of autonomous adaptation leads to economic impacts below 0.10% of GDP until half of the century (i.e., $1^\circ C$ warming), representing a 66% decrease in losses with only planned adaptation. The combination of planned and autonomous adaptation brings down the costs of climate change at the end of the century from 2% under the no adaptation scenario to about 1% of GDP.

Throughout the century the synergistic effects between autonomous and planned adaptation are positive and lead to adaptation levels much higher than those attained only with planned adaptation alone and higher than those obtained with independent

autonomous and planned adaptation (Figure 8.4b). In general, autonomous adaptation reduces the optimal level of planned adaptation and the associated costs (figures 8.4c and 8.4d). In the case when synergistic effects are taken into account, the optimal planned adaptation level is low for the first half of the century but it increases rapidly afterwards. At the end of the century, the planned adaptation attains higher levels than when autonomous adaptation is ignored. In this case, the optimal investment in adaptation at the end of the century is higher than in any other case. This is due to the assumption that synergistic effects expand the range of autonomous adaptation when planned adaptation increases, making adaptation cheaper.

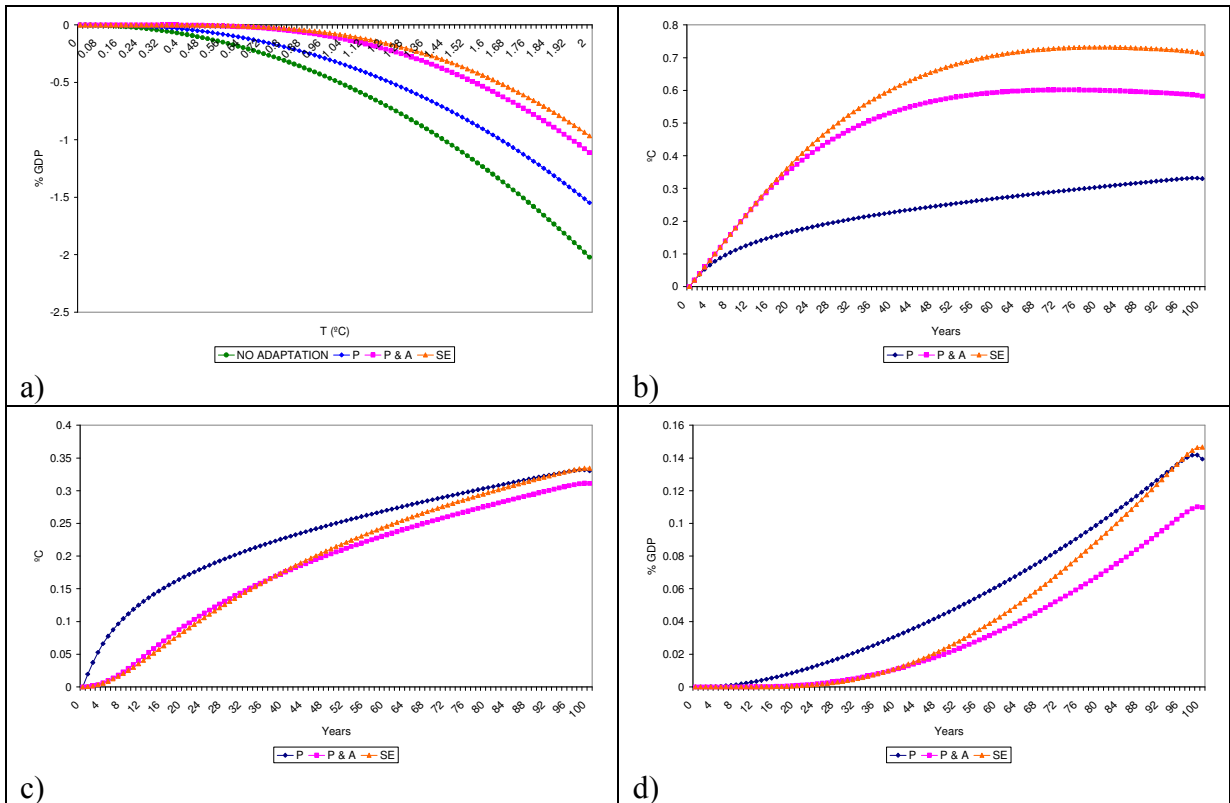


Figure 8.4. Effects of autonomous adaptation on economic losses, adaptation levels and costs for $T_i = 2^\circ C$ and high sensitivity. Panel a) economic losses as percent of global GDP for the following cases: no adaptation (green), planned adaptation (blue; P), planned and autonomous adaptation (fuchsia; P & A), and synergistic effects (orange; SE). Panel b) total adaptation level a_t for P (blue), P & A (fuchsia) and SE (orange). Panel c) planned adaptation for P (blue), P & A (fuchsia) and SE (orange). Panel e) adaptation costs AD_t for P (blue), P & A (fuchsia) and SE (orange).

Figure 8.5 shows that the effects of autonomous adaptation (whether synergistic effects are taken into account or not) are limited for higher warming scenarios. The differences in the total level of adaptation (Figure 8.5b) between planned, planned and autonomous and planned and autonomous with synergistic effects start decreasing for warming above 1.5°C. For increases in T_t larger than 5°C, the total adaptation depends mostly on the chosen planned adaptation level (Figure 8.5c). The largest differences in adaptation costs due to the inclusion autonomous adaptation occur at the end of the century and when synergistic effects are allowed (about 0.15% of GDP). Results suggest that the most important contribution of autonomous adaptation is restricted to moderate warming. For larger increases in T_t , the gains from autonomous adaptation in terms of avoided impacts are small.

It is important to take into account that these results are incomplete since what is being analyzed here is the behavior of the proposed impact function, not a full IAM, and therefore mitigation (and its interaction with adaptation) is outside the scope of the present analysis.

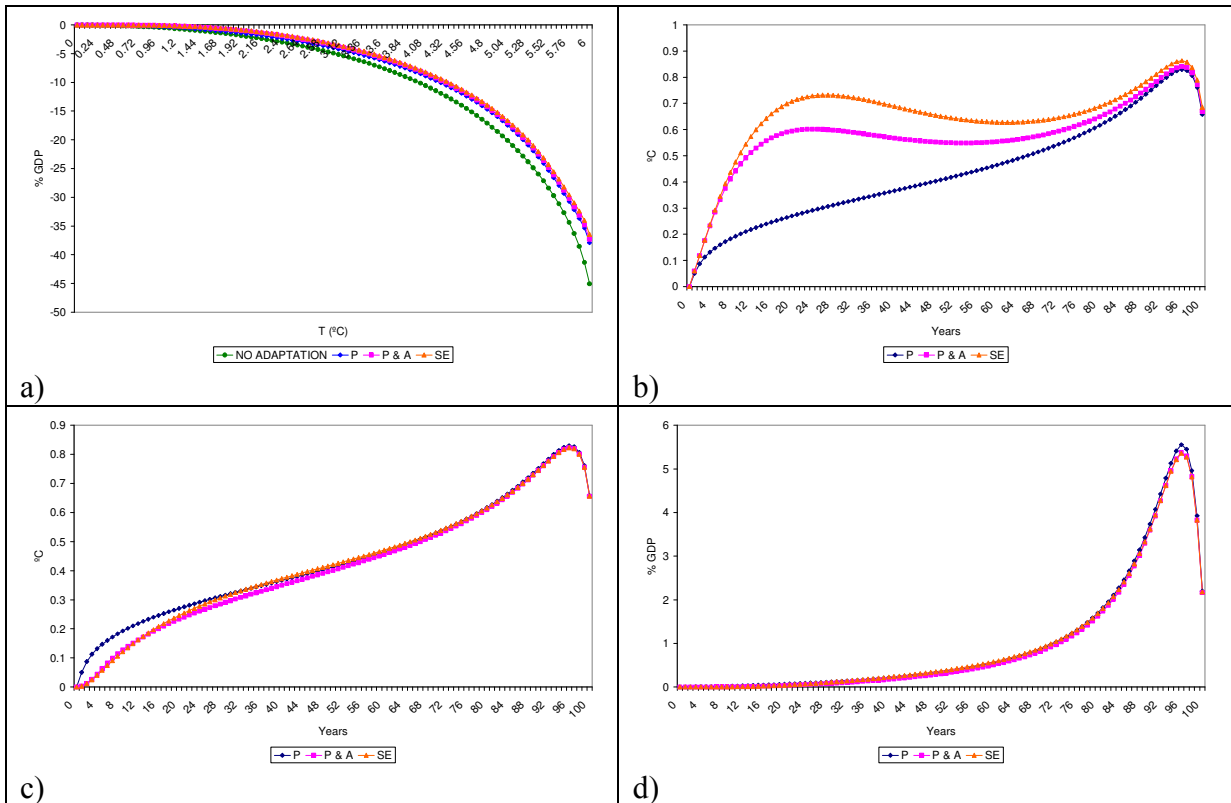


Figure 8.5. Effects of autonomous adaptation on economic losses, adaptation levels and costs for $T_t = 6^\circ C$ and high sensitivity. Panel a) economic losses as percent of global GDP for the following cases: no adaptation (green), planned adaptation (blue; P), planned and autonomous adaptation (fuchsia; P & A), and synergistic effects (orange; SE). Panel b) total adaptation level a_t for P (blue), P & A (fuchsia) and SE (orange). Panel c) planned adaptation for P (blue), P & A (fuchsia) and SE (orange). Panel e) adaptation costs AD_t for P (blue), P & A (fuchsia) and SE (orange).

8.4 Conclusions

While a limited number of impact functions for IAMs explicitly model adaptation, the links between impacts, adaptation efforts and the system's sensitivity has been seldom explored or modeled. In this chapter we present a generalized impact function that allows feedbacks and interactions between impacts, autonomous and planned adaptation and vulnerability by explicitly modeling adaptation and sensitivity as dynamic processes. The proposed generalizations not only can emulate the behavior of the impact functions included in some of the most commonly used IAMs but, through dynamic sensitivity, it provides a mechanism for the type of highly nonlinear impacts for large changes in

climate that has been recently discussed in the literature. Contrary to most of the current impact functions, this new type of impact function maps economic losses in terms of the time-varying capacity of a system to deal with climate conditions experienced at a certain period in time, instead of fixed proportional damages produced by absolute changes in climate. Future extensions include analyzing the interactions between adaptation and mitigation policies for optimal climate policy under different emissions scenarios, discount rates and utility function specifications.

Appendix E

E1. RICE2007 impact functions.

Regional impact functions can be obtained by scaling the parameters of the global function as follows:

$$D_{r,t} = \frac{\alpha_{1,g}}{\varpi_r \sigma_g} T_t + \frac{\alpha_{2,g}}{(\varpi_r \sigma_g)^{\alpha_3}} T_t^{\alpha_3} = \alpha_{1,r} T_t + \alpha_{2,r} T_t^{\alpha_3} \quad (\text{E.1})$$

where the subscripts g and r denote global and regional parameters, respectively. ϖ_r is a scaling parameter such that $\varpi_r \sigma_g = \sigma_r$, i.e., it represents the quantity that the global coping range needs to be multiplied to obtain the regional coping range. The values for the scaling parameter were obtained by minimizing the sum of squared differences between the original regional functions in RICE2007 (Nordhaus 2008; Nordhaus and Boyer 2000; values reproduced in Table E1) and equation (E.1) using the parameter values of DICE2007.

Table E1. Scaling factors and Root Mean Square Error estimates for the regional impact functions.

	US	EU	Japan	Russia	Eurasia	China	India	ME	Africa	LA	OHI	Other
ϖ_r	1.42	1.34	1.33	1.57	1.48	1.42	1.06	1.16	1.04	1.39	1.35	1.17
RMSE	0.00	0.00	0.00	0.00	0.00	0.07	0.39	0.25	0.30	0.05	0.00	0.16

Half of the regions have a RMSE of zero, indicating that the regional parameters have been perfectly matched by adjusting the scaling factor ϖ_r (Table E1). The other six (China, India, Middle East, Africa, Latin America and Other) have a much higher RMSE between 0.05% and 0.39% of GDP. Unlike the others, the optimal climate of these regions is not that of the reference period (i.e., 1900) but a cooler climate. That is, in these cases the quadratic function is shifted by a constant. To take into account this characteristic, the optimization problem was extended to allow the optimum climate to be different from zero:

$$D_{r,t} = \frac{\alpha_{1,g}}{\varpi_r \sigma_g} (T_t + c) + \frac{\alpha_{2,g}}{(\varpi_r \sigma_g)^{\alpha_3}} (T_t + c)^2 \quad (\text{E.2})$$

Table E2 shows that once the optimal temperature is not restricted to be zero, the original RICE2007 results are reproduced closely for these regions with a very small RMSE. The values of c may be interpreted as a measure of adaptation deficit in comparison with the globe and other regions. These regions are not fully adapted to the reference climate. For these regions the adjusted impact functions imply small impacts for the reference climate, being larger for the regions that have larger values of c like India (0.89°C), Middle East (0.67°C) and Africa (0.66°C).

Table E2. Scaling factors, distance to optimum and Root Mean Square Error estimates for regions with optimal temperatures different to that of the reference period.

	China	India	ME	Africa	LA	Other
ϖ_r	1.50	1.24	1.31	1.17	1.45	1.27
C	0.28	0.89	0.67	0.66	0.21	0.43
RMSE	0.00	0.07	0.03	0.04	0.00	0.01

E2. Supplementary figures

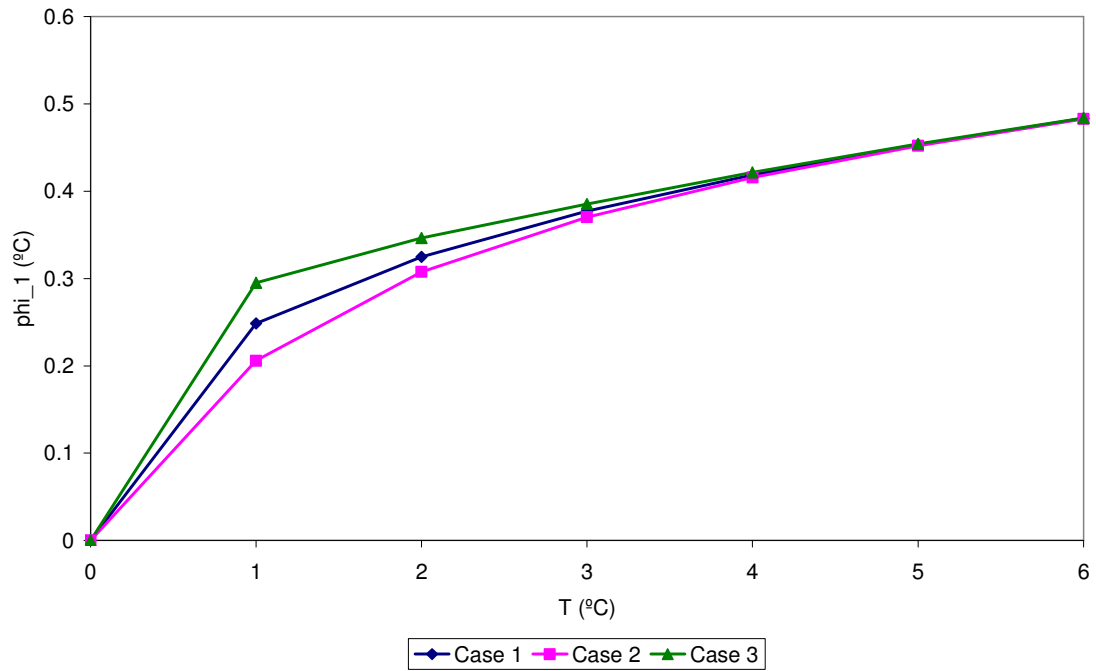


Figure E1. Optimal levels of planned adaptation ϕ_1 for increases from 0°C to 6°C in global temperatures in 1°C steps. Case 1 includes only planned adaptation; Case 2 includes planned and autonomous adaptation; Case 3 allows for synergistic effects between planned and autonomous adaptation. Parameter values: $\alpha_3 = 2$, $\sigma = 0.345$, $\beta_1 = 0$, $\beta_2 = 0.0045$, $\lambda_1 = 11.71$, $\lambda_2 = 4$.

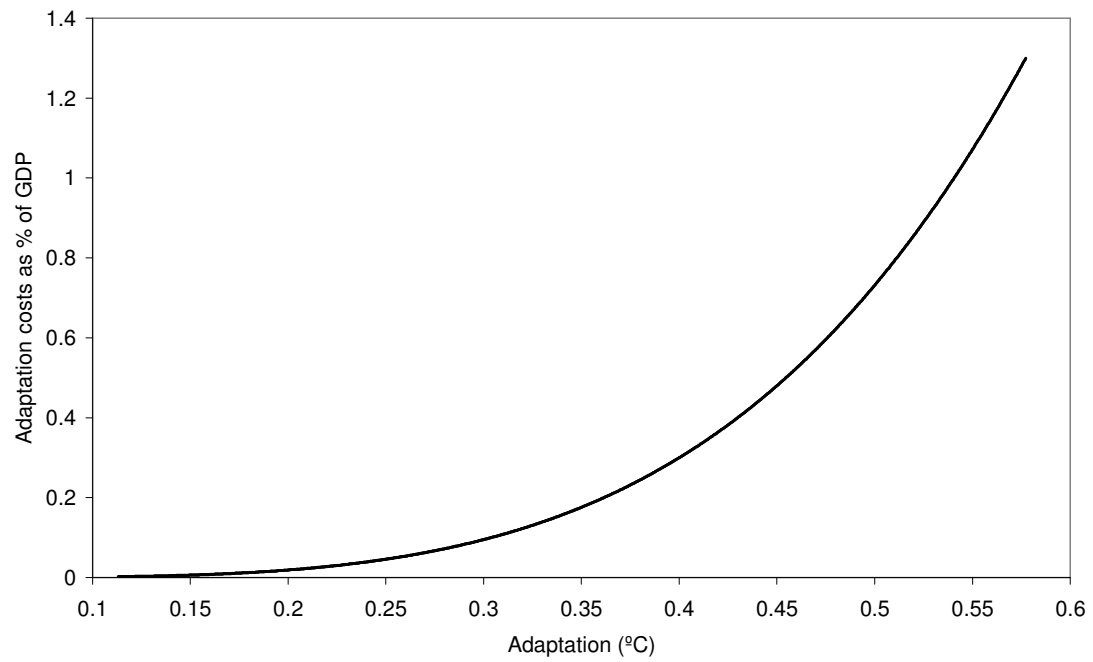


Figure E2. Adaptation costs as percent of global GDP as a function of the adaptation level in °C.

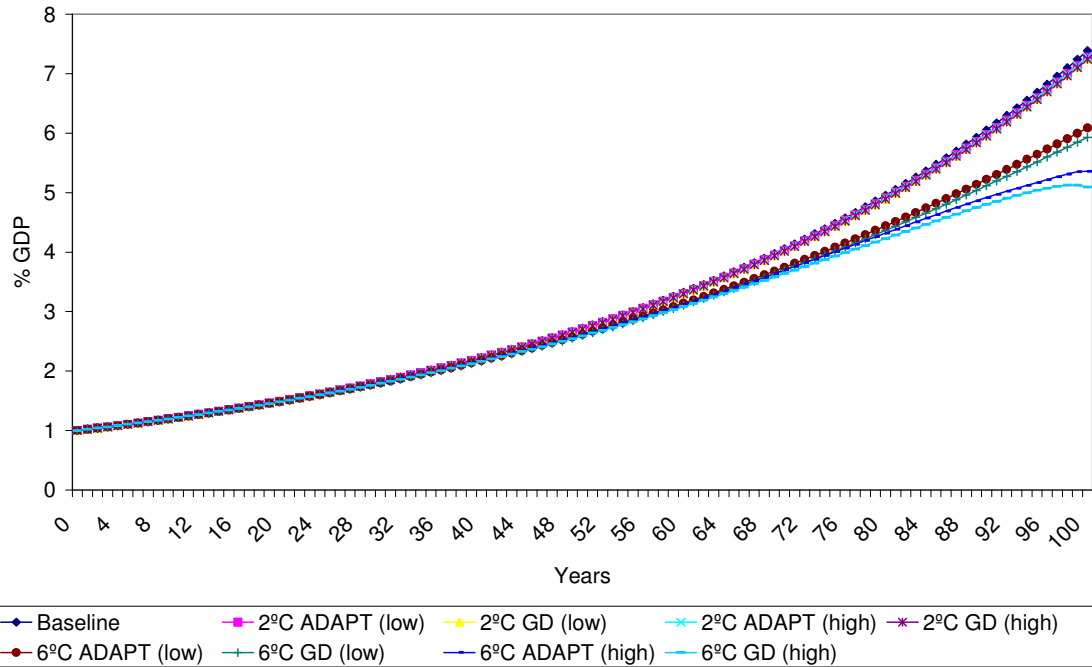


Figure E3. GDP projections for the scenarios: baseline (blue line with diamond); $T_t = 2^\circ C$, low sensitivity and adaptation (pink line with square); $T_t = 2^\circ C$, low sensitivity (yellow line with triangle); $T_t = 2^\circ C$, high sensitivity and adaptation (light blue line with cross); $T_t = 2^\circ C$, high sensitivity (purple line with cross and dot); $T_t = 6^\circ C$, low sensitivity and adaptation (brown line with dot); $T_t = 6^\circ C$, low sensitivity (light blue line with marker); $T_t = 6^\circ C$, high sensitivity and adaptation (blue line); $T_t = 6^\circ C$, high sensitivity (light blue line).